THE JOURNAL OF PHYSICAL CHEMISTRY B

Article

pubs.acs.org/JPCB

Molecular Events in Lamin B1 Homopolymerization: A Biophysical Characterization

Pritha Bhattacharjee, Dipak Dasgupta, and Kaushik Sengupta*

Biophysics and Structural Genomics Division, Saha Institute of Nuclear Physics, 1/AF Bidhannagar, Kolkata-700064, India

Supporting Information

ABSTRACT: Lamin B1 is one of the major constituents of the nuclear lamina, a filamentous network underlying the nucleoplasmic side of the inner nuclear membrane. Homopolymerization of lamin B1, coupled to the homotypic and heterotypic association of other lamin types, is central to building the higher order network pattern inside the nucleus. This in turn maintains the mechanical and functional integrity of the lamina. We have characterized the molecular basis of the self-association of lamin B1 using spectroscopic and calorimetric methods. We report that concentration dependent lamin B1 oligomerization involves significant alterations in secondary and tertiary structures of the protein resulting in fairly observable compaction in size. Comparison of the energetics of the homotypic association of lamin B1 with that of lamin A reported earlier led to the finding that lamin A oligomers had higher thermodynamic stability. This leads us to conjecture that lamin B1 has less stress bearing ability compared to lamin A.

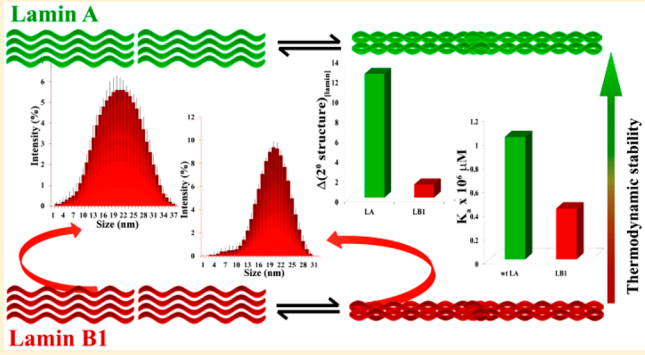

INTRODUCTION

Lamin proteins are major constituents of the fibrous lamina underlying the inner nuclear envelope of metazoan cells.[1,2] Lamins are classified into A and B types according to their molecular mass, sequence homology, and expression pattern. A-type lamins include lamin A and C that are alternate splice variants of the *LMNA* gene;[3] minor isoforms include lamin AΔ10[4] and lamin C2.[5] Lamin B1 and B2 are the two B-type lamins encoded by two different genes *LMNB1* and *LMNB2*.[6] The B-type lamins are ubiquitously expressed in all cells in contrast to the differentially regulated expression of lamin A.[7,8] Lamin B3 is a minor splice variant of the *LMNB2* gene, expressed only in germline.[6] The nuclear lamins possess a tripartite structure typical of intermediate filament proteins, comprising a short unstructured N-terminal head and a relatively long C-terminal tail domain flanking a central rod domain[9] (Figure 1). A stretch of 108 amino acid residues in the tail domain of lamins forms a β-barrel structure akin to that of immunoglobulin,[10−12] hence the name Ig fold. The rod domain of the protein is α-helical, bearing heptad repeats of amino acid residues that form coiled-coiled structures, the basic building blocks in the higher order assembly of nuclear lamins.[10,13] The high structural similarity of the A- and B-type lamins (55% sequence identity in the case of human lamin A, B1, and B2; Supporting Information Table 1 and Figure S1) allows them to follow similar assembly pathways under *in vitro* conditions. This involves the end-on overlap of the parallel coiled-coil dimeric lamin units to form octamers, known as protofilaments, which undergo further oligomerization and compaction to form 10 nm filaments.[14,15] However, differences in primary structures of the proteins eventually make them functionally distinct. The B-type lamins are more acidic and remain closely associated with the inner nuclear membrane compared to the A-type lamins.[6,16] Furthermore, the nucleoplasmic pool of B-type lamins is less soluble and immobile in contrast to the soluble and mobile lamin A/C population.[17−19] The A- and B-type lamins have been reported to form distinct networks within the nucleus, by electron microscopy, confocal microscopy, and very recently by superresolution microscopy.[19−21] However, these networks have been shown to interact among themselves by fluorescence correlation spectroscopy (FCS) and fluorescence resonance energy transfer (FRET) studies.[19,22] This arrangement of segregated, interacting networks hints at distinct properties of the A- and B-type lamin homopolymers in maintaining the structural and functional integrity of the nuclear lamina. Mutations in lamins cause a number of human diseases collectively termed as laminopathies, the underlying mechanisms of which remain largely undefined.[23−25] The A-type lamins are involved in more than 16 different diseased phenotypes. On the contrary, B-type lamins have been linked to just two diseased conditions. Duplication of the lamin B1 gene causes adult-onset autosomal dominant leukodystrophy (ADLD),[26] and duplication of the *LMNB2* gene is associated with acquired partial lipodystrophy (APL).[27] Lamin B1 is

Received: July 29, 2015
Revised: October 13, 2015
Published: October 14, 2015

ACS Publications © 2015 American Chemical Society

DOI: 10.1021/acs.jpcb.5b07320
J. Phys. Chem. B 2015, 119, 14014−14021

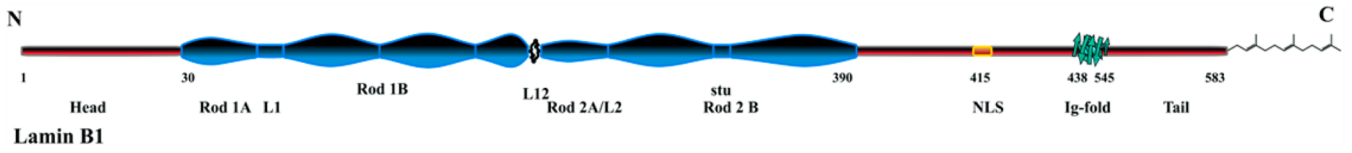

Figure 1. Schematic representation of the tripartite structure of lamin B1. A short, unstructured N-terminal "head" domain is followed by a central α-helical rod and a C-terminal "tail" domain. The C-terminal tail domain contains the nuclear localization signal (NLS), the β-barrel Ig-fold domain, and the −CAAX box.[28] The residue numbers indicate the start of the rod, start of the tail domain, initial residue of the NLS, start and end of the Ig-fold, and the end of the tail along with the farnesyl group, respectively.

thought to be fundamental for the functioning of the nucleus for its role in structural organization, gene expression, transcriptional regulation, nucleolar plasticity, senescence, cell proliferation, and survival.[28−34] These findings prompted us to study the molecular events preceding the higher order oligomerization of lamin B1. We have addressed this question by biophysical studies on heterologously expressed lamin B1 protein. In this report we have used spectroscopic techniques to analyze the concentration dependent self-association of lamin B1. Fluorescence, circular dichroism, and dynamic light scattering allowed us to elucidate the secondary and tertiary components that are involved in the self-association of lamin B1. Isothermal titration calorimetry was employed to address the thermodynamics, in turn probing the molecular basis of the process. Our studies have shown that lamin B1 undergoes molecular association involving structural modulation and appreciable compaction with increasing concentration.

EXPERIMENTAL METHODS

Molecular Cloning. Human lamin B1 was cloned into the pET-17b vector from pEGFP-human lamin B1 (a gift from Prof. R. D. Goldman, Northwestern University, Feinberg School of Medicine, Chicago, IL). Forward (5′-GGGAATTC-**CATATG**GAATTCATGGCGACTGCGACCCCCGTGC-3′) and reverse (5′-CCG**CTCGAG**CGGTTACATAATTGC-ACAGCTTCTATTGGATGC-3′) primers were used to amplify the full-length lamin B1 gene by PCR with Phusion High-Fidelity DNA Polymerase (Thermo Scientific Inc., USA) and insert *Nde*I and *Xho*I sites into the sequence, respectively. The vector and the inserts were digested as per the manufacturer's protocol overnight at 37 °C with *Nde*I (New England Biolabs (NEB), U.K.) and *Xho*I (NEB, U.K.), added sequentially in a gap of 5 h. The digested products were ligated at 16 °C overnight; successful cloning was confirmed by colony PCR as well as by the sequencing of positive clones.

Protein Expression and Purification. Heterologous expression of lamin B1 from the pET-17b vector was carried out in BL21(DE3) pLysS (Novagen) grown in 2xYT medium (Himedia) by inducing with 2 mM IPTG. Cells were aerated for 2 h postinduction at 37 °C. The inclusion bodies obtained on lysing the cell pellets were solubilized in 6 M urea, 25 mM Tris-HCl pH 8.5, and 1 mM DTT. These were then purified using a Resource-Q (1 mL, GE Healthcare) column in a linear NaCl gradient. Protein fractions purified to near homogeneity were concentrated by acetone precipitation, dissolved in 6 M urea, 25 mM Tris-HCl pH 8.5, 250 mM NaCl, and 1 mM DTT, and renatured by the stepwise removal of urea as required for subsequent experimentation.[35] Renaturation of the protein was also confirmed by obtaining the CD spectra of the protein at different steps of the dialyzing process (Figure S2). Protein concentrations were checked in a Cecil 7500 UV−visible spectrophotometer by the Bradford method before and after experimentation. The protein concentrations before and after performing the experiments varied within an error limit of 5%. This eliminated the possibility of phasing out of lamin by nonspecific aggregation during the experiments. All experiments were carried out in 25 mM Tris-HCl pH 8.5, 250 mM NaCl, and 1 mM DTT named as the working buffer (WB), unless otherwise stated, and buffers and proteins were filtered through 0.1 μm Millex Syringe Filters (Millipore) and thoroughly centrifuged at 13,000 rpm to remove any nonspecific protein aggregates in the form of insoluble precipitates. The identity of the protein was checked by immunoblotting with rabbit polyclonal anti-human lamin B1 antibody (Abcam, ab16048).[36]

Circular Dichroism (CD). Far-UV CD spectra of lamin B1 were recorded over a concentration range of 0.2 to 8 μM in WB at 25 °C in a Jasco J-720 spectropolarimeter with a quartz cuvette having a path length of 1 mm. All spectra were normalized to molar ellipticity values and were smoothed using the Adjacent Averaging algorithm of Origin 8 Pro. The corresponding molar ellipticity values at 222 nm and the ratio of the observed ellipticity values at 222 and 208 nm were plotted against the input protein concentrations. The CD spectra and the corresponding plots represented here are the average of three independent experiments.

Steady State Fluorescence Spectroscopy. Fluorescence spectra of lamin B1 were recorded in a PerkinElmer LS 55 luminescence spectrometer at an excitation wavelength of 295 nm, keeping both excitation and emission slit widths at 5 nm. The experiment was performed at 25 °C using 1 cm path length quartz cuvettes (Hellma). All spectra were normalized with respect to *N*-acetyl-L-tryptophanamide (Sigma-Aldrich), which was used as an example for completely exposed tryptophan residues. Such normalization helps to characterize the environment of the internal reporter, tryptophan residue(s) and can thereby be employed to follow the structural alteration associated with the oligomerization of lamin.

The concentration of 4,4-bis(1-anilinonaphthalene 8-sulfonate) (bis-ANS), obtained from Molecular Probes Inc., dissolved in freshly distilled dimethyl sulfoxide (Fluka) was determined in methanol in a Cecil 7500 UV−visible spectrophotometer (ε_{395} in methanol = 23000 M^{-1} cm^{-1}).[37] Emission spectra of 1 and 6 μM bis-ANS alone and in the presence of 1 and 6 μM lamin B1 were recorded as stated above at an excitation wavelength of 399 mm.

Dynamic Light Scattering (DLS). Dynamic light scattering measurements of different concentrations of lamin B1 in the WB at 25 °C were carried on in a Zetasizer Nano S particle analyzer (Malvern Instruments, U.K.), equipped with a 4 mW He−Ne laser (632.8 nm) as the light source, the detector being placed at a fixed angle of 173°. A correlation curve was generated from the intensity autocorrelation function, $G(\tau) = A[1 + B\exp(-2\Gamma\tau)]$, where G is the correlation coefficient, A is

DOI: 10.1021/acs.jpcb.5b07320
J. Phys. Chem. B 2015, 119, 14014−14021

the amplitude of the correlation function, and B is the baseline. The Stokes−Einstein diffusion coefficient (D) was obtained from the relation $\Gamma = Dq^2$, where q is the scattering vector. Cumulant analysis of the correlation curve was used to obtain the intensity percentage statistics distribution by the inbuilt software and the mean hydrodynamic diameters at the position of maximum intensity (percentage).

The measurements were performed using quartz cuvettes in volumes of 45 μL with 1 and 4 μM protein solutions. Stock protein solutions and buffers were filtered through Millex GV 0.1 μm syringe filter units (Millipore) and thoroughly degassed, prior to experimentation. The data obtained are averages of 10 measurements of 15 s, each being run 10 times.

Isothermal Titration Calorimetry (ITC). Thermodynamics of the homotypic association of lamin B1 was studied by isothermal titration calorimetry (ITC). Twenty microliters of a 35 μM protein stock was injected in the single injection method (SIM) into a 50 nM protein solution in 25 mM Tris-HCl and 250 mM NaCl pH 8.5, such that the final concentration of the protein in the cell was 3.5 μM. The experiment was carried out at 25 °C in a MicroCal iTC$_{200}$ microcalorimeter, the stirring speed being kept at 400 rpm. The titration profile as obtained from the above experimentation was fitted into the single set of binding site model of the inbuilt MicroCal iTC$_{200}$ SIM software by the Levenberg−Marquardt nonlinear least-squares curve fitting algorithm. The diluted protein (50 nM), believed to be in the deoligomerized state, was considered to be the macromolecule having a bulk concentration of M_t in the active cell volume V_0. 35 μM of the proteins, considered to be the ligand, having bulk and free concentrations of X_t and $[X]$ in the same active cell volume respectively, were bound to the deoligomerized proteins. The apparent association constant (K_a) is given by

$$K_a = \frac{\theta}{(1-\theta)[X]}$$

where θ is the fraction of sites occupied by the ligand. The bulk concentration of the ligand is given by

$$X_t = [X] + n\theta M_t$$

where n is the number of binding sites. The total heat content of the solution within the active cell volume, V_0, is

$$Q = n\theta M_t \Delta H V_0$$

ΔH being the molar heat of binding. The heat release associated with the ith injection, considering to accompany the change in volume ΔV_i, is given by

$$\Delta Q_i = Q_i + \frac{dV_i}{V_0}\left[\frac{Q_i + Q_{i-1}}{2}\right] - Q_{i-1}$$

Binding entropy was obtained from

$$\Delta G = -RT \ln K_a = \Delta H - T\Delta S$$

where R is the universal gas constant and T is the temperature at which the experiment was performed. All buffer and protein solutions were filtered using Millex GV 0.1 μm syringe driven filter units (Millipore) and thoroughly degassed by centrifuging at 13,000 rpm at 25 °C for 30 min prior to experimentation. A necessary criterion for studying the thermodynamics of a process by ITC is its reversibility. In this case, we checked the reversibility of the oligomerization process by performing the foregoing concentration dependent studies in both directions. Two separate sets of experiments were performed, one by increasing the concentration and the other by the dilution of the protein. The reversibility of the oligomerization process also ruled out the possibility of nonspecific protein aggregates that might be formed by lamin B1.

RESULTS

Protein Expression and Purification. Robust expression of human lamin B1 was obtained from *E. coli* in 2xYT medium by the induction with 2 mM IPTG. Proteins were purified to near homogeneity by ion-exchange chromatography (Figure 2A). The protein was renatured from 6 M urea, 25 mM Tris-HCl pH 8.5, 250 mM NaCl, and 1 mM DTT by dialyzing out urea in steps of two according to the standard protocol for purification of lamins[35] (Figure S2). Subsequent experiments were performed in 25 mM Tris-HCl pH 8.5, 250 mM NaCl, and 1 mM DTT (WB), in which the lamins have been reported to undergo specific oligomerization.[14,35] The protein was further confirmed to be human lamin B1 from the clean bands obtained on probing with anti-human lamin B1 antibody (Figure 2B).

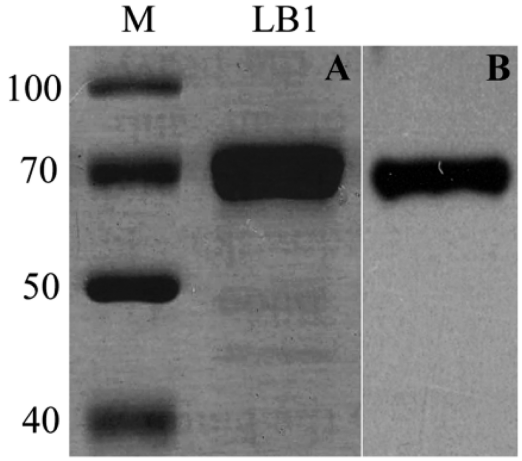

Figure 2. Characterization of human lamin B1 (LB1) overexpressed in BL21(DE3) pLysS. (A) Analysis of Resource-Q purified lamin B1 on a 10% SDS−PAGE; M denotes the molecular weight marker (kDa). (B) Immunoblot of the purified protein by rabbit polyclonal anti-human lamin B1 antibody (ab16048).

Secondary Structural Modulations Accompany the Self-Association of Lamin B1. Figure 3A illustrates the CD spectra at two representative concentrations of 0.4 μM and 4 μM of lamin B1. The notable features emerging from a comparison of the two spectra suggest that there is a reduction in the molar ellipticity values with the increase in concentration. Concomitant with the decrease in molar ellipticity, there is a change in the ratio of ellipticity values at 222 and 208 nm at two concentrations. Plot of molar ellipticity at 222 nm as a function of concentration of lamin B1 shows a break corresponding to 1.3 (±0.02) μM indicative of a change in the state of association of the protein beyond this concentration (Figure 3B). An inverse relationship exists between the molar ellipticity and the protein concentration. There is also concentration dependent, nonlinear decrease in the ratio of the ellipticity values at 222 and 208 nm ($\theta_{222}/\theta_{208}$) suggesting an alteration in the nature of the helix (Figure 3C). It may be noted that the concentrations corresponding to the break-points in the titration curves (Figure 3B and Figure 3C) are

DOI: 10.1021/acs.jpcb.5b07320
J. Phys. Chem. B 2015, 119, 14014−14021

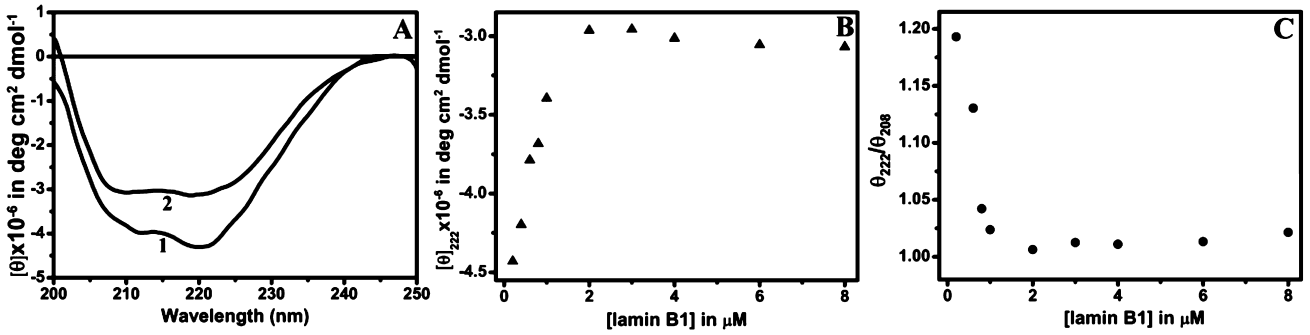

Figure 3. Circular dichroism spectroscopy for the self-associating lamin B1. (A) CD spectra of lamin B1 at two representative concentrations of 0.4 (1) and 4 (2) μM recorded in 25 mM Tris-HCl pH 8.5, 250 mM NaCl, and 1 mM DTT at 25 °C. (B) Plot of molar ellipticity of lamin B1 at 222 nm against its input concentration and (C) plot of the ratio of the observed ellipticity at 222 and 208 nm as a function of the concentration of lamin B1 derived from the CD spectra of lamin B1 recorded in the concentration ranges of 0.2−8 μM (spectra of lamin B1 at all measured concentrations have been represented in Figure S3).

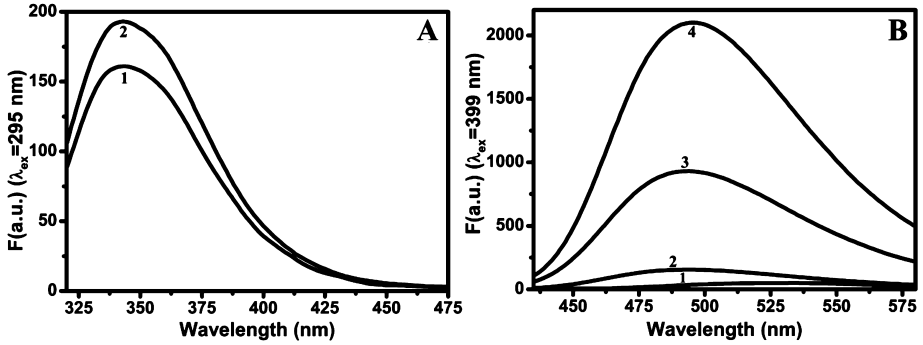

Figure 4. Steady state fluorescence indicating self-association of lamin B1. (A) Tryptophan fluorescence of 1 μM lamin B1 multiplied by four (1) and 4 μM lamin B1 (2). (B) Emission spectrum of 6 μM bis-ANS in the presence (4) and absence (1) of 6 μM lamin B1; this was compared with the emission spectrum of 1 μM bis-ANS in the presence of 1 μM lamin B1 (2) multiplied by six (3). All spectra were acquired in 25 mM Tris-HCl pH 8.5, 250 mM NaCl, and 1 mM DTT at 25 °C.

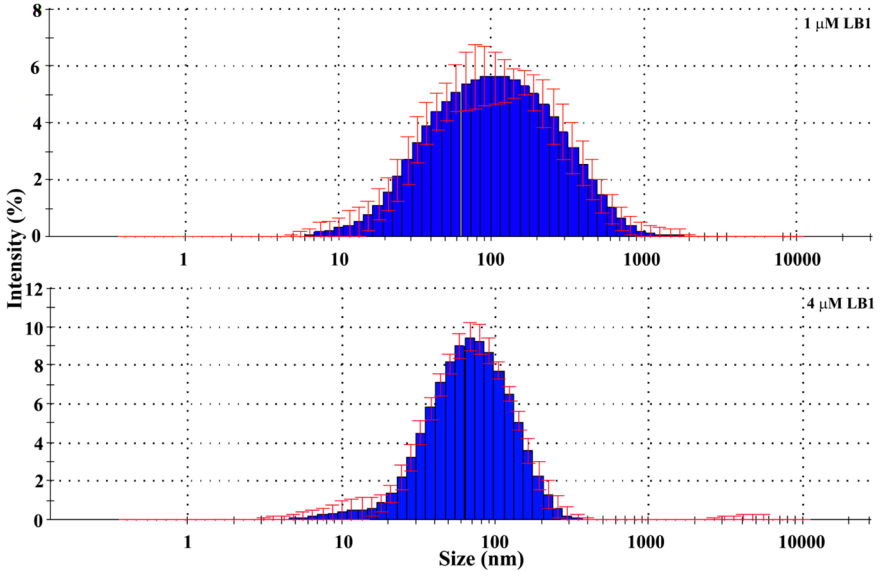

Figure 5. Dynamic light scattering of lamin B1 (LB1). Intensity percentage statistical distribution of 1 μM and 4 μM lamin B1 in 25 mM Tris-HCl and 250 mM NaCl pH 8.5 measured at 25 °C.

comparable. This might originate from the antiparallel arrangement of the protein moieties upon self-association.

Self-Association Implicated in Tertiary Structural Components of Lamin B1. Nonoverlap of the fluorescence spectra of 4 μM lamin B1 and 1 μM lamin B1 multiplied by four (Figure 4A) indicates a nonlinearity in the concentration dependent fluorescence intensity of lamin B1. This observation further supports the oligomerization of lamin B1 in this concentration range as observed from circular dichroism spectroscopy. Fluorescence intensity of the protein in the

DOI: 10.1021/acs.jpcb.5b07320
J. Phys. Chem. B 2015, 119, 14014−14021

oligomerized state is higher than that in the individual units. Therefore, the overall environment of the Trp residues is altered with oligomerization.

Hydrophobic patches on the surface of lamin B1 have been probed with the extrinsic fluorescence reporter, bis-ANS (Figure 4B). Addition of 6 μM lamin B1 to an equimolar amount of bis-ANS results in a blue shift of 34 nm to the emission maximum of bis-ANS (spectrum 4, Figure 4B). This is accompanied by a 42-fold enhancement in fluorescence intensity at λ_{max}. A 3-fold increase in intensity and a 36 nm blue shift of emission maximum are observed on adding 1 μM lamin B1 to 1 μM bis-ANS (spectrum 2, Figure 4B). Spectrum 4 has been compared with six times the spectrum 2 (spectrum 3). The nonoverlap of spectra 1 and 3 proposes a concentration dependent alteration in the number/nature of hydrophobic pockets on lamin B1 upon oligomerization, a sequel to increase in concentration from 1 μM to 6 μM. There is a marked increase in the hydrophobic patches of the protein in the self-associated form (6 μM). Thus, nature and organization of the hydrophobic patches on the protein surface are different for different concentrations of the protein.

Lamin B1 Forms Homogeneous Globular Oligomers. Results of dynamic light scattering (DLS) conform to the observations from the fluorescence experiments. The position and nature of the intensity percentage statistical distribution (PSD) as a function of the hydrodynamic diameter differed significantly with the concentration of lamin B1 (Figure 5). A broad distribution of hydrodynamic diameter corresponding to a position of maximum intensity at 105 (±5) nm is acquired for 1 μM lamin B1. Increase in the protein concentration (4 μM) results in a considerably narrow histogram while the position of maximum intensity shifts to 68 (±2) nm. The polydispersity index (pdi) obtained from DLS is a measure of the heterogeneity of the system studied. In the present study, pdi decreased from 0.5 to 0.2 on increasing the protein concentration from 1 to 4 μM. Thus, a gross alteration in the shape and size of the protein corresponding to its tertiary structure occurs upon increasing its concentration. This is again indicative of an alteration in its state of association, in accordance with the previous observations.

Energetics of the Self-Association of Lamin B1. Thermodynamics of the self-association of lamin B1 has been studied by isothermal titration calorimetry (ITC) in the single injection method (SIM). Injecting 20 μL of 35 μM lamin B1 to a 50 nM lamin B1 solution leads to an initial dilution followed by a progressive association of the protein to a concentration of 3.5 μM. The thermogram (Figure 6) and associated thermodynamic parameters show that the oligomerization of lamin B1, as studied here, is an endothermic process. Lamin B1 associates with a K_d value of 2.3 (±0.02) μM. A favorable ΔG value (−7.7 kcal mol^{-1}) results from positive entropy (438 cal mol^{-1} deg^{-1}) and enthalpy (123 ± 3.1 kcal mol^{-1}) values. This is indicative of the release of water molecules and/or ions and the effect of configurational entropy on interaction of deoligomerized lamin B1 units to form oligomers. ITC results also show that nine molecules of lamin B1 associate to form oligomeric units (N = 9 ± 0.3) at higher concentrations.

DISCUSSION

Optimal expression and polymerization of lamin B1 is a key step in the formation of a functional lamina. It has been previously reported that nuclear lamins, particularly lamin A/C, oligomerize within concentrations of 0.1−0.2 mg/mL.[36,38]

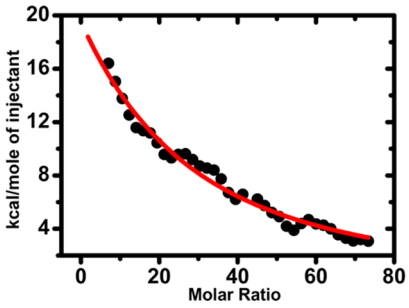

Figure 6. Thermodynamics of the self-association of lamin B1. Thermogram obtained from the isothermal titration calorimetry of lamin B1 in 25 mM Tris-HCl and 250 mM NaCl; pH 8.5 at 25 °C. Twenty microliters of 35 μM lamin B1 solution in the syringe was injected to a 50 nM lamin B1 solution in the cell so that the final concentration of the protein was 3.5 μM.

However, similar studies with lamin B1 are hitherto unknown. Taking cues from these results we have characterized the structural basis of the self-association of full-length lamin B1 using biophysical techniques. The results indicate that alterations in the secondary and tertiary structures of the protein accompany the aggregation.

As evident from the molar ellipticity vs concentration plot of lamin B1 over the concentration range of 0 to 8 μM, an alteration of secondary structure accompanies the self-association of the lamin. The break-point, corresponding to 1.3 μM lamin B1, suggests that higher order oligomers with decreased magnitude of molar ellipticity are progressively formed with increase in concentration. This might originate from the antiparallel arrangement of the head-to-tail oligomers of the protein.[39] In interacting α-helices, the band at 222 nm corresponding to the n → π^* transition is polarized.[40] Thus, we have plotted the ratio of the ellipticity values at 222 and 208 nm as a function of concentration of the protein. This parameter shows an increase in the population of interacting helices with increasing protein concentrations.[40] Interestingly, inflection points in the concentration dependence of both $[\theta]_{222}$ and $\theta_{222}/\theta_{208}$ are coincident. The coincidence provides further evidence for an alteration in the nature of the helix on self-association at higher concentrations.

The secondary structural modulations of lamin B1 on aggregation are manifested in its tertiary structural components studied by fluorescence spectroscopy. Intrinsic tryptophan fluorescence of the protein shows increased quantum yield in higher concentrations of the protein. Thus, the electronic environment of the Trp residues reorients such that the surrounding water molecules, amino acid residues, and amide bonds lead to relatively less quenching of Trp fluorescence in the self-associated forms. Notably, all Trp residues map in the highly conserved Ig-fold domain of the protein. Thus, alteration in their fluorescence properties might result from an end-on overlap of the lamin B1 moieties implicated in their *in vitro* association.[15] This again may be responsible for the Trp residues coming into contact with other residues of the N-terminal head or rod 1A of the protein. Hence, a shift in the overall tertiary structural disposition of the oligomeric protein is manifested in its Trp fluorescence.

Concentration dependent alteration in the tertiary structure of the protein is further corroborated from interaction of the protein with bis-ANS. Bis-ANS interacts with hydrophobic pockets on a protein surface. As a result, fluorescence

DOI: 10.1021/acs.jpcb.5b07320
J. Phys. Chem. B 2015, 119, 14014−14021

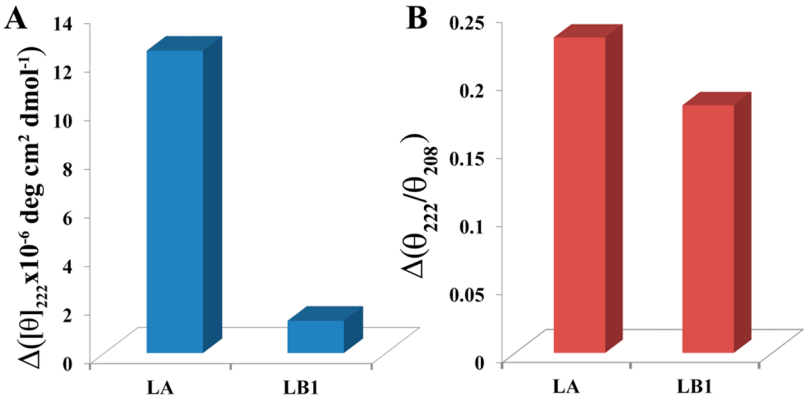

Figure 7. Comparison of the concentration dependent circular dichroism of lamin A (LA) and lamin B1 (LB1). Difference in the magnitude of (A) molar ellipticity at 222 nm of 4 and 0.2 μM lamin A and lamin B1 and (B) the ratio of the ellipticity values at 222 and 208 nm of 0.2 and 4 μM lamin A and lamin B1.

quenching of the molecule due to charge transfer in a polar environment is decreased. Again, an apolar environment stabilizes its ground state and destabilizes its excited state resulting in a blue shift in its emission maximum. The fluorescence intensity of bis-ANS is increased significantly on adding higher concentrations of the protein. This can be ascribed to interacting protein surfaces in the oligomers that expel water molecules to form hydrophobic pockets, accessible to bis-ANS. Thus, hydrophobic forces might play a role in the aggregation of lamin B1.

Ordering of the protein units displacing water molecules is again evident from the entropy driven oligomerization of lamin B1 studied by isothermal titration calorimetry. The reversible oligomerization of lamin B1 can be described by the equilibrium

$$n(\mathrm{LB}) \leftrightharpoons (\mathrm{LB})_n$$

where LB denotes one molecule of full length human lamin B1 and n denotes the number of molecules of lamin B1 that associate to form one oligomer, i.e., the degree of oligomerization of the protein. The deoligomerization followed by the progressive association of the lamin B1 molecules in the calorimetric cell is an endothermic process; oligomerization proceeds with a micromolar dissociation constant, and the number of monomers in the oligomer is nine, as suggested from the stoichiometry in ITC experiments. The degree of association obtained is coherent with the protofilaments formed in the *in vitro* association of B-type lamins visualized by electron microscopy.[14,41]

Interestingly, from DLS measurements we find that the protein undergoes a compaction along with a narrowing of the intensity PSD profile on oligomerization. Broad distribution profiles at lower concentrations might be originating from cylindrical or longitudinal protein bundles. These bundles further oligomerize and get compacted to form near globular structures.

Thus, we can summarize that full length human lamin B1 undergoes oligomerization within the concentration range of 0.2−8 μM. This homoploymeric association of lamin B1 involves head-to-tail and lateral ordering of the protein units involving hydrophobic interactions. Nevertheless, the self-association of lamin B1 is thermodynamically favorable because of the breaking of ionic and water structure implicated in the ordering and compaction of the lamin B1 molecules.

Comparison of the Homotypic Interaction of Lamin A and Lamin B1. The self-association of lamin proteins, also termed as their homotypic interaction, is the key factor in maintaining the structural organization of the nuclear lamina. The nuclear lamina in mammalian cells is made up of anastomosed, interacting, homopolymeric networks of A- and B-type lamins.[19,22] Nonetheless, the expression patterns of A- and B-type lamins are tissue specific.[42] B-type lamins are considered to be more fundamental to the nucleus as they are present right from embryogenesis. Moreover, most invertebrates possess just one lamin gene, which is a B-type lamin.[2] Localization of B-type lamins in the nucleus is primarily restricted to the nuclear membrane. Lamin A, on the other hand, has both nucleoplasmic and laminar localization. This is because of differential post-translational modifications of A- and B-type lamins.[28] Lamins, with the exception of lamin C, bear a conserved C-terminal sequence known as the −CAAX box. Both A- and B-type lamins get farnesylated at the −CAAX box; B-type lamins retain the farnesyl group whereas it is removed by further post-translational modifications in mature lamin A. As a result, lamin B1 is reported to form a stiff network within the nucleus.[43] In a recent report, Swift et al. showed that expression levels of lamin B1 and lamin A depend upon the rigidity of the tissue. Lamin B1 is abundant in soft tissues that bear less mechanical stress such as brain, bone marrow, and fat, whereas lamin A expression levels are higher in tissues that are rigid and bear high stress levels such as muscles, cartilages, and bones. Lamin A expression induces stiffness and stability of the nuclear lamina in terms of resistance to mechanical stress. Furthermore, lamin A levels enhance extracellular matrix elasticity-directed differentiation of mesenchymal stem cells.[44] *In vitro* viscoelastic studies show a high resilience or solid-like behavior for lamin B1 networks that stiffen under shear and can bear high strain amplitudes before disruption.[45] However, similar viscoelastic studies from our group demonstrated that lamin A networks behaved more like fluids and could resist ∼2.5 times the strain of lamin B1 networks before rupturing.[46] Phosphorylation of the nuclear lamins is a major player in their conformation, solubility, and hence supramolecular organization within the nucleus. Phosphorylation induced depolymerization of lamins drives the disassembly of the nuclear lamina during mitosis.[47−50] Stress induced (stiff matrix) reduction in phosphorylation levels of lamin A renders it insoluble, in turn strengthening the nuclear lamina. Stiffer matrix again induces overexpression of lamin A that adds to the thickening and

DOI: 10.1021/acs.jpcb.5b07320
J. Phys. Chem. B 2015, 119, 14014−14021

additional stability of the nuclear lamina. Expression and phosphorylation levels of lamin B1, on the other hand, do not vary significantly with matrix elasticity.[44] Thus, lamin A homopolymeric networks prove to be the major stress bearing elements that maintain the mechanostability of the nucleus. Nevertheless, soft tissues like nucleated blood cells show large variations in lamin B1 levels.[51] Therefore, lamin B1 might play a significant role in modulating and maintaining the nuclear lamina of soft tissues and undifferentiated cells where lamin A is absent.[51,52] Consequently, it is important to characterize the inherent homopolymeric behavior of both A- and B-type lamins. Earlier studies comparing the homotypic association of lamins led to ambiguous results.[16,53−55] Hence, from this study along with a previous report from our lab,[36] we have characterized and compared the homotypic association of lamin A and lamin B1. It is interesting to note that the affinity for the homotypic association of lamin A as obtained from ITC experiments (K_d = 0.97 ± 0.06 μM) is ∼2-fold higher than that for lamin B1 (K_d = 2.3 ± 0.02 μM). Thus, oligomers of lamin A are thermodynamically more stable than the oligomers of lamin B1. Nonetheless, at equal concentrations, the number of lamin A and B1 molecules that associate remain similar. Furthermore, concentration dependent circular dichroism studies indicate a lower inflection point for the self-association of lamin A (0.76 ± 0.06 μM) compared to lamin B1 (1.3 ± 0.02 μM). Such differences in the stability of lamin A and B1 oligomers could be ascribed to dissimilarity in the secondary structures of the associating proteins. The magnitude of decrease in molar ellipticity at 222 nm with increase in concentrations for lamin A is ∼9 times the decrease for lamin B1 (Figure 7A). Concentration dependent alteration in the helicity, as illustrated by the $\theta_{222}/\theta_{208}$ ratio, for lamin A is again higher than that for lamin B1 (Figure 7B). However, the exact correlation of such secondary structural alterations to the thermodynamic stability of lamin filaments needs detailed structural elucidations of the full-length proteins. Nonetheless, inflection points obtained from $[\theta]_{222}$ vs concentration plots reinforce to the higher association constant and stability of the lamin A oligomers than that of lamin B1. Therefore, we propose that the inherent higher propensity of lamin A to self-associate helps to maintain stable, rigid lamin A fibers manifested in their high stress-bearing ability. Likewise, the inherent instability of the lamin B1 filaments might be the cause of lower levels of lamin B1 being expressed in tissues experiencing limited mechanical stress.

■ ASSOCIATED CONTENT

Supporting Information

The Supporting Information is available free of charge on the ACS Publications website at DOI: 10.1021/acs.jpcb.5b07320.

Sequence alignment and CD spectra (PDF)

■ AUTHOR INFORMATION

Corresponding Author

*Tel: 91-33-2337 5345 ext 3504. E-mail: kaushik.sengupta@saha.ac.in.

Notes

The authors declare no competing financial interest.

■ ACKNOWLEDGMENTS

We acknowledge financial support from MMDDA and BARD intramural project grants of The Department of Atomic Energy, Government of India.

■ REFERENCES

(1) Cohen, M.; Lee, K. K.; Wilson, K. L.; Gruenbaum, Y. Transcriptional repression, apoptosis, human disease and the functional evolution of the nuclear lamina. *Trends Biochem. Sci.* **2001**, *26*, 41−47.

(2) Melcer, S.; Gruenbaum, Y.; Krohne, G. Invertebrate lamins. *Exp. Cell Res.* **2007**, *313*, 2157−2166.

(3) Lin, F.; Worman, H. J. Structural organization of the human gene encoding nuclear lamin A and nuclear lamin C. *J. Biol. Chem.* **1993**, *268*, 16321−16326.

(4) Machiels, B. M.; Zorenc, A. H. G.; Endert, J. M.; Kuijpers, H. J. H.; van Eys, G. J. J. M.; Ramaekers, F. C. S.; Broers, J. L. V. An alternative splicing product of the lamin A/C gene lacks exon 10. *J. Biol. Chem.* **1996**, *271*, 9249−9253.

(5) Furukawa, K.; Inagaki, H.; Hotta, Y. Identification and cloning of an mRNA coding for a germ cell-specific A-type lamin in mice. *Exp. Cell Res.* **1994**, *212*, 426−430.

(6) Peter, M.; Kitten, G.; Lehner, C.; Vorburger, K.; Bailer, S.; Maridor, G.; Nigg, E. Cloning and sequencing of cDNA clones encoding chicken lamins A and B1 and comparison of the primary structures of vertebrate A-and B-type lamins. *J. Mol. Biol.* **1989**, *208*, 393−404.

(7) Stewart, C.; Burke, B. Teratocarcinoma stem cells and early mouse embryos contain only a single major lamin polypeptide closely resembling lamin B. *Cell* **1987**, *51*, 383−392.

(8) Rober, R.; Weber, K.; Osborn, M. Differential timing of nuclear lamin A/C expression in the various organs of the mouse embryo and the young animal: a developmental study. *Development* **1989**, *105*, 365−378.

(9) Parry, D.; Conway, J. F.; Steinert, P. M. Structural studies on lamin. Similarities and differences between lamin and intermediate-filament proteins. *Biochem. J.* **1986**, *238*, 305−308.

(10) Ruan, J.; Xu, C.; Bian, C.; Lam, R.; Wang, J.-P.; Kania, J.; Min, J.; Zang, J. Crystal structures of the coil 2B fragment and the globular tail domain of human lamin B1. *FEBS Lett.* **2012**, *586*, 314−318.

(11) Krimm, I.; Östlund, C.; Gilquin, B.; Couprie, J.; Hossenlopp, P.; Mornon, J. P.; Bonne, G.; Courvalin, J. C.; Worman, H. J.; Zinn-Justin, S. The Ig-like structure of the C-terminal domain of lamin A/C, mutated in muscular dystrophies, cardiomyopathy, and partial lipodystrophy. *Structure* **2002**, *10*, 811−823.

(12) Dhe-Paganon, S.; Werner, E. D.; Chi, Y. I.; Shoelson, S. E. Structure of the globular tail of nuclear lamin. *J. Biol. Chem.* **2002**, *277*, 17381−17384.

(13) Strelkov, S. V.; Schumacher, J.; Burkhard, P.; Aebi, U.; Herrmann, H. Crystal structure of the human lamin A coil 2B dimer: implications for the head-to-tail association of nuclear lamins. *J. Mol. Biol.* **2004**, *343*, 1067−1080.

(14) Heitlinger, E.; Peter, M.; Häner, M.; Lustig, A.; Aebi, U.; Nigg, E. Expression of chicken lamin B2 in Escherichia coli: characterization of its structure, assembly, and molecular interactions. *J. Cell Biol.* **1991**, *113*, 485−495.

(15) Stuurman, N.; Sasse, B.; Fisher, P. A. Intermediate filament protein polymerization: molecular analysis of *Drosophila* nuclear lamin head-to-tail binding. *J. Struct. Biol.* **1996**, *117*, 1−15.

(16) Georgatos, S. D.; Stournaras, C.; Blobel, G. Heterotypic and homotypic associations between the nuclear lamins: site-specificity and control by phosphorylation. *Proc. Natl. Acad. Sci. U. S. A.* **1988**, *85*, 4325−4329.

(17) Broers, J.; Machiels, B. M.; Van Eys, G.; Kuijpers, H.; Manders, E.; van Driel, R.; Ramaekers, F. Dynamics of the nuclear lamina as monitored by GFP-tagged A-type lamins. *J. Cell Sci.* **1999**, *112*, 3463−3475.

(18) Moir, R. D.; Yoon, M.; Khuon, S.; Goldman, R. D. Nuclear Lamins a and B1 Different Pathways of Assembly during Nuclear Envelope Formation in Living Cells. *J. Cell Biol.* **2000**, *151*, 1155−1168.

(19) Shimi, T.; Pfleghaar, K.; Kojima, S.-i.; Pack, C.-G.; Solovei, I.; Goldman, A. E.; Adam, S. A.; Shumaker, D. K.; Kinjo, M.; Cremer, T. The A- and B-type nuclear lamin networks: microdomains involved in

DOI: 10.1021/acs.jpcb.5b07320
J. Phys. Chem. B 2015, 119, 14014−14021

chromatin organization and transcription. *Genes Dev.* **2008**, *22*, 3409−3421.
(20) Goldberg, M. W.; Huttenlauch, I.; Hutchison, C. J.; Stick, R. Filaments made from A-and B-type lamins differ in structure and organization. *J. Cell Sci.* **2008**, *121*, 215−225.
(21) Shimi, T.; Kittisopikul, M.; Tran, J.; Goldman, A. E.; Adam, S. A.; Zheng, Y.; Jaqaman, K.; Goldman, R. D. Structural organization of nuclear lamins A, C, B1 and B2 revealed by super-resolution microscopy. *Mol. Biol. Cell* **2015**, DOI: 10.1091/mbc.E15-07-0461.
(22) Delbarre, E.; Tramier, M.; Coppey-Moisan, M.; Gaillard, C.; Courvalin, J.-C.; Buendia, B. The truncated prelamin A in Hutchinson−Gilford progeria syndrome alters segregation of A-type and B-type lamin homopolymers. *Hum. Mol. Genet.* **2006**, *15*, 1113−1122.
(23) Worman, H. J. Nuclear lamins and laminopathies. *J. Pathol.* **2012**, *226*, 316−325.
(24) Zaremba-Czogalla, M.; Dubińska-Magiera, M.; Rzepecki, R. Laminopathies: the molecular background of the disease and the prospects for its treatment. *Cell. Mol. Biol. Lett.* **2011**, *16*, 114−148.
(25) Worman, H. J.; Bonne, G. Laminopathies": a wide spectrum of human diseases. *Exp. Cell Res.* **2007**, *313*, 2121−2133.
(26) Padiath, Q. S.; Saigoh, K.; Schiffmann, R.; Asahara, H.; Yamada, T.; Koeppen, A.; Hogan, K.; Ptáček, L. J.; Fu, Y.-H. Lamin B1 duplications cause autosomal dominant leukodystrophy. *Nat. Genet.* **2006**, *38*, 1114−1123.
(27) Hegele, R. A.; Cao, H.; Liu, D. M.; Costain, G. A.; Charlton-Menys, V.; Rodger, N. W.; Durrington, P. N. Sequencing of the reannotated LMNB2 gene reveals novel mutations in patients with acquired partial lipodystrophy. *Am. J. Hum. Genet.* **2006**, *79*, 383−389.
(28) Dechat, T.; Pfleghaar, K.; Sengupta, K.; Shimi, T.; Shumaker, D. K.; Solimando, L.; Goldman, R. D. Nuclear lamins: major factors in the structural organization and function of the nucleus and chromatin. *Genes Dev.* **2008**, *22*, 832−853.
(29) Malhas, A.; Lee, C. F.; Sanders, R.; Saunders, N. J.; Vaux, D. J. Defects in lamin B1 expression or processing affect interphase chromosome position and gene expression. *J. Cell Biol.* **2007**, *176*, 593−603.
(30) Tang, C. W.; Maya-Mendoza, A.; Martin, C.; Zeng, K.; Chen, S.; Feret, D.; Wilson, S. A.; Jackson, D. A. The integrity of a lamin-B1-dependent nucleoskeleton is a fundamental determinant of RNA synthesis in human cells. *J. Cell Sci.* **2008**, *121*, 1014−1024.
(31) Martin, C.; Chen, S.; Maya-Mendoza, A.; Lovric, J.; Sims, P. F.; Jackson, D. A. Lamin B1 maintains the functional plasticity of nucleoli. *J. Cell Sci.* **2009**, *122*, 1551−1562.
(32) Dreesen, O.; Chojnowski, A.; Ong, P. F.; Zhao, T. Y.; Common, J. E.; Lunny, D.; Lane, E. B.; Lee, S. J.; Vardy, L. A.; Stewart, C. L. Lamin B1 fluctuations have differential effects on cellular proliferation and senescence. *J. Cell Biol.* **2013**, *200*, 605−617.
(33) Shimi, T.; Butin-Israeli, V.; Adam, S. A.; Hamanaka, R. B.; Goldman, A. E.; Lucas, C. A.; Shumaker, D. K.; Kosak, S. T.; Chandel, N. S.; Goldman, R. D. The role of nuclear lamin B1 in cell proliferation and senescence. *Genes Dev.* **2011**, *25*, 2579−2593.
(34) Harborth, J.; Elbashir, S. M.; Bechert, K.; Tuschl, T.; Weber, K. Identification of essential genes in cultured mammalian cells using small interfering RNAs. *J. Cell Sci.* **2001**, *114*, 4557−4565.
(35) Moir, R. D.; Donaldson, A. D.; Stewart, M. Expression in Escherichia coli of human lamins A and C: influence of head and tail domains on assembly properties and paracrystal formation. *J. Cell Sci.* **1991**, *99* (Part 2), 363−372.
(36) Bhattacharjee, P.; Banerjee, A.; Banerjee, A.; Dasgupta, D.; Sengupta, K. Structural alterations of lamin A protein in dilated cardiomyopathy. *Biochemistry* **2013**, *52*, 4229−4241.
(37) Slavik, J. Anilinonaphthalene sulfonate as a probe of membrane composition and function. *Biochim. Biophys. Acta, Rev. Biomembr.* **1982**, *694*, 1−25.
(38) Aebi, U.; Cohn, J.; Buhle, L.; Gerace, L. The nuclear lamina is a meshwork of intermediate-type filaments. *Nature* **1986**, *323*, 560−564.
(39) Dittmer, T. A.; Misteli, T. The lamin protein family. *Genome Biol.* **2011**, *12*, 222.
(40) Lau, S.; Taneja, A.; Hodges, R. Synthesis of a model protein of defined secondary and quaternary structure. Effect of chain length on the stabilization and formation of two-stranded alpha-helical coiled-coils. *J. Biol. Chem.* **1984**, *259*, 13253−13261.
(41) Heitlinger, E.; Peter, M.; Lustig, A.; Villiger, W.; Nigg, E.; Aebi, U. The role of the head and tail domain in lamin structure and assembly: analysis of bacterially expressed chicken lamin A and truncated B2 lamins. *J. Struct. Biol.* **1992**, *108*, 74−91.
(42) Broers, J. L.; Machiels, B. M.; Kuijpers, H. J.; Smedts, F.; van den Kieboom, R.; Raymond, Y.; Ramaekers, F. C. A-and B-type lamins are differentially expressed in normal human tissues. *Histochem. Cell Biol.* **1997**, *107*, 505−517.
(43) Panorchan, P.; Wirtz, D.; Tseng, Y. Structure-function relationship of biological gels revealed by multiple-particle tracking and differential interference contrast microscopy: the case of human lamin networks. *Phys. Rev. E* **2004**, *70*, 041906.
(44) Swift, J.; Ivanovska, I. L.; Buxboim, A.; Harada, T.; Dingal, P. D. P.; Pinter, J.; Pajerowski, J. D.; Spinler, K. R.; Shin, J.-W.; Tewari, M. Nuclear lamin-A scales with tissue stiffness and enhances matrix-directed differentiation. *Science* **2013**, *341*, 1240104−1240115.
(45) Panorchan, P.; Schafer, B. W.; Wirtz, D.; Tseng, Y. Nuclear envelope breakdown requires overcoming the mechanical integrity of the nuclear lamina. *J. Biol. Chem.* **2004**, *279*, 43462−43467.
(46) Banerjee, A.; Rathee, V.; Krishnaswamy, R.; Bhattacharjee, P.; Ray, P.; Sood, A. K.; Sengupta, K. Viscoelastic behavior of human lamin A proteins in the context of dilated cardiomyopathy. *PLoS One* **2013**, *8*, e8341.
(47) Gerace, L.; Blobel, G. The nuclear envelope lamina is reversibly depolymerized during mitosis. *Cell* **1980**, *19*, 277−287.
(48) Burke, B.; Gerace, L. A cell free system to study reassembly of the nuclear envelope at the end of mitosis. *Cell* **1986**, *44*, 639−652.
(49) Heald, R.; McKeon, F. Mutations of phosphorylation sites in lamin A that prevent nuclear lamina disassembly in mitosis. *Cell* **1990**, *61*, 579−589.
(50) Peter, M.; Nakagawa, J.; Doree, M.; Labbe, J.; Nigg, E. In vitro disassembly of the nuclear lamina and M phase-specific phosphorylation of lamins by cdc2 kinase. *Cell* **1990**, *61*, 591−602.
(51) Olins, A. L.; Herrmann, H.; Lichter, P.; Kratzmeier, M.; Doenecke, D.; Olins, D. E. Nuclear envelope and chromatin compositional differences comparing undifferentiated and retinoic acid-and phorbol ester-treated HL-60 cells. *Exp. Cell Res.* **2001**, *268*, 115−127.
(52) Young, S. G.; Jung, H.-J.; Lee, J. M.; Fong, L. G. Nuclear lamins and neurobiology. *Mol. Cell. Biol.* **2014**, *34*, 2776−2785.
(53) Krohne, G.; Wolin, S.; McKeon, F.; Franke, W.; Kirschner, M. Nuclear lamin LI of Xenopus laevis: cDNA cloning, amino acid sequence and binding specificity of a member of the lamin B subfamily. *EMBO J.* **1987**, *6*, 3801−3808.
(54) Ye, Q.; Worman, H. J. Protein-protein interactions between human nuclear lamins expressed in yeast. *Exp. Cell Res.* **1995**, *219*, 292−298.
(55) Schirmer, E. C.; Gerace, L. The stability of the nuclear lamina polymer changes with the composition of lamin subtypes according to their individual binding strengths. *J. Biol. Chem.* **2004**, *279*, 42811−42817.

DOI: 10.1021/acs.jpcb.5b07320
J. Phys. Chem. B 2015, 119, 14014−14021